Optical Review (2021) 28:145–158
https://doi.org/10.1007/s10043-021-00645-9

REGULAR PAPER

Range-restricted pixel difference global histogram equalization for infrared image contrast enhancement

Jianjun Wang[1,2] · Yi Li[1] · Lihua Cao[1] · Yan Li[1] · Ning Li[1] · HuiBin Gao[1]

Received: 14 September 2020 / Accepted: 13 January 2021 / Published online: 3 February 2021

Abstract
Histogram equalization (HE)-based technology has been widely applied in infrared image contrast enhancement due to its effectiveness and simple implementation. However, HE and its variations considered the accumulation of pixels in different gray values, thus ordinarily result in artifact effects, over-enhancement and noise amplification, especially in the uniformity region. In this paper, we redefine and formulate a new HE technology to overcome the shortcomings of traditional HE technology. 2D difference information between two adjacent pixels is introduced for infrared image histogram calculation and its calculation is achieved by a reasonable difference threshold. With the purpose of adaptability to different scenes, the display range of output image is controlled by 2D difference information. To preserve detail edges, we apply adaptive plateau HE on 2D difference information-related histogram. Experiments and results show that the proposed algorithm has better scene adaptability and outperforms other compared algorithms by enhancing the contrast without introducing over-enhancement effect.

Keywords Infrared image · Contrast enhancement · Histogram equalization · 2D difference information

1 Introduction

Infrared imaging technology can detect thermal radiation, which is invisible for human visual system, has been widely used in military and civilian surveillance. Images obtained from the infrared imaging system are often characterized by low contrast and blurred texture details, due to thermals isotropy radiation and the uneven photosensitive response of infrared sensor. Thus, infrared images contrast enhancement is a vital step in the application of infrared imaging technology and has attracted the attention of many researchers [1–3].

To improve the quality of infrared images and gain a satisfied visual experience, numerous infrared image enhancement methods have been proposed. Double plateau histogram equalization (DPHE) controls the infrared image over-enhancement by an upper threshold and enhances details with a lower threshold [3]. Wavelet transform-based algorithm enhances image global and local information under appropriate parameter selection [4]. Multi-scale decomposition algorithm based on bilateral filtering and guided filtering achieves infrared image detail information enhancement [5]. High-frequency detail information and low-frequency information contrast in infrared image get enhancement using Retinex and wavelet transform [6]. Details and texture information get enhanced using the total variation-based method in infrared image gradient domain. Other commonly used infrared image enhancement algorithms are based on fuzzy theory, neural networks, (non-down sampled contourlet transform) NSCT, top hat transforms, and so on [7–10].

Among these existed infrared image enhancement algorithms, conventional global histogram equalization (HE) remains one of the most popular techniques for its simple implementation and satisfactory performance in contrast enhancement. The HE technique performs input-to-output mapping by a cumulative distribution function (CDF) of the input image histogram. The mapping leads to gray levels with large groups of pixels to be expanded to occupy a larger range of gray levels in the output image, while pixels of other gray level ranges are compressed to a smaller range.

✉ Yi Li
leey2009@sina.com

[1] Changchun Institute of Optics, Fine Mechanics and Physics, Chinese Academy of Sciences, Changchun 130033, China

[2] University of Chinese Academy of Sciences, Beijing 100039, China

As a result, the performance of HE in the output image is over-enhancement and noise amplification in the uniformity region, if there are large peaks in the histogram of the input image. To handle the problem mentioned above, a lot of HE-based technologies have been developed and improved. Plateau histogram equalization (PHE) is proposed to constrain background noise amplification, but detail information enhancement is limited. Double-plateau histogram equalization (DPHE) is then produced. An upper threshold is used to constrain background noise and a lower threshold aims to protect and enhance the details [3]. Local histogram equalization (LHE) equalizes each histogram in a small window, by sliding through each window sequentially, instead of the histogram of the entire image [11]. Brightness preserving Bi-Histogram Equalization (BBHE) attempts to solve the problem of brightness preservation and splits the image histogram into two histograms and equalizes them independently using the mean value of the input image [12]. Contrast Limited Adaptive Histogram Equalization (CLAHE) is introduced to restrict contrast enhancement and reduce the problem of noise amplification [13]. Though these HE-based algorithms improve the overall image contrast effectively, they still suffer from over-enhancement and noise amplification in the uniformity region as they ignore the relationship between adjacent pixels in the image and try to process 2D images using 1D accumulation information.

Recently, several algorithms have been proposed to calculate the histogram of neighboring pixel values for contrast enhancement [14–18]. Contextual and variational contrast enhancement algorithm (CVC) achieves contrast enhancement by introducing a 2D histogram and modifying it to emphasize large gray level differences [14]. Layered difference representation (LDR) attempts to amplify gray-level differences that frequently occur in the input image to enhance the contrast and overcome over-enhancement [17]. Advanced gradient histogram equalization with sine function (SAGHE) realizes gradient enhancement and contrast enhancement by introducing an advanced gradient histogram and control the enhancement level of gradient histogram equalization. 2D histogram-based algorithms make great progress in suppressing over-enhancement in uniformity region [18]. However, noise amplification and over-enhancement are still existed, due to the overuse of display range.

In this paper, our goal is to develop a new histogram-based infrared image enhancement algorithm, which is capable of enhancing image contrast without over-enhancement and has good adaptability to different scenes. First, we obtain a 2D information-related 1D histogram by calculating the difference information between adjacent pixels in a 4-adjacency neighborhood with a difference threshold. Then different image scenes are quantified by difference information calculation, and the display range for output image is gained from an established quantitative function. Finally, adaptive plateau histogram equalization is introduced to protect tinny details and textures. We conduct a series of experiments, and the experimental results demonstrate that the proposed algorithm has better scene adaptability and outperforms other compared algorithms by enhancing the contrast without introducing the over-enhancement effect. Our main contributions in this paper are as follows:

(1) 2D difference information histogram for infrared image contrast enhancement is proposed to overcome over-enhancement and noise amplification in uniformity region.

(2) To control the degree of infrared image enhancement, scenarios are distinguished by difference information-based feature pixels and display range for each output image is restricted by the number of feature pixels.

The remainder of this paper is designed as follows: in Sect. 2, the mechanism of the proposed algorithm is introduced; experiments and related discussion are detailed in Sect. 3; in Sect. 4, we give a conclusion of the paper.

2 Range-restricted pixel difference histogram equalization (RRPDHE)

The proposed algorithm not only aims to eliminate the artifact effects and over-enhancement in HE-based technology, but also achieve better contrast enhancement and scene adaptability for infrared images. Figure 1 summarizes the framework of the proposed range-restricted pixel difference histogram equalization. The main processes are divided into

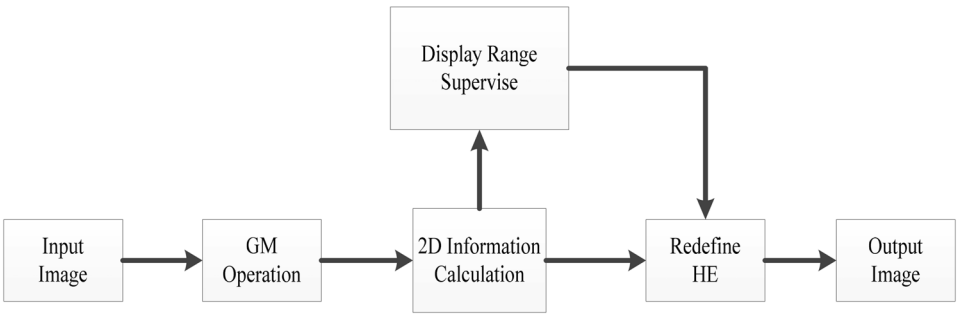

Fig. 1 The framework of RRPDHE

four parts, and each part will be introduced in the following subsections.

2.1 2D difference information

Conventional HE uses the calculation of gray values of each pixel in an infrared image and applies the calculation probability to remap new gray values for the output image. Obviously, it results in artifact effects and amplification of random noise in uniformity region. The main reason is that pixel calculation probabilities in uniformity region are higher than other pixels, and larger gray value range is assigned to describe the uniformity region in output image. As a result, the artifact effects and random noise are more noticeable than they are in input image.

To deal with such kind of drawback of HE-based technology, the proposed algorithm employs 2D difference information between adjacent pixels instead of simple accumulation of different pixel values. 2D difference information depicts the relationship between pixels. 2D difference information accumulation $\mathbf{H}_D$ calculates the difference between each pixel and neighboring pixels in the entire infrared image.

$$\mathbf{H}_D = \{h(x)|0 \le x \le L-1\}, \tag{1}$$

h(x) is the gray-level statistical histogram, which counts the number of pixels with gray-level x in the image, and x is the grayscale of a pixel in the infrared image.$L = 2^{\text{pixel}depth}$ is the full display range gray value, for 8-bit output infrared image $L = 2^8 = 256$.

To get 2D information, we run a gradient mask (GM) operation firstly. There are many optional GM methods in the conventional method, such as Sobel, Prewitt and so on [17]. With the purpose of presenting the authentic relationship between pixels and the simplicity of calculation, we use a four-neighbor gradient mask operation. The result of each direction alone is an element of difference vector $\nabla\mathbf{d}$, as show in (2).

$$\begin{cases} \nabla_r(m,n) = |I(m+1,n) - I(m,n)| \\ \nabla_l(m,n) = |I(m-1,n) - I(m,n)| \\ \nabla_u(m,n) = |I(m,n+1) - I(m,n)| \\ \nabla_d(m,n) = |I(m,n-1) - I(m,n)| \end{cases}. \tag{2}$$

Difference vector $\nabla\mathbf{d}$ gets further standardization to one or zero by a difference threshold T_d. One of the elements in $\nabla\mathbf{d}$ is calculated as follows:

$$\nabla \mathrm{d}_{m-1,n} = Std(\frac{\nabla_l(m,n)}{\mathrm{T}_d}), \tag{3}$$

$$\mathrm{T}_d \in [1, L-1], \tag{4}$$

$$Std(\frac{a}{b}) = \begin{cases} 1 & a \ge b \\ 0 & else \end{cases}, \tag{5}$$

$Std()$ is a standardized function.T_d is a variable value determined experimentally and shows the deviation of uniformity region in original infrared images. The method to choose a suitable T_d will be introduced in the following description. After GM operation and difference vector standardization, 2D difference information-based histogram $\mathbf{H}_D$ is achieved by counting pixels in related difference vectors.

$$h(x) \leftarrow h(x) + \mathrm{num}(\nabla\mathbf{d}), \tag{6}$$

x is the gray value of each pixel in infrared image. num() counts how many 1′s are in vector $\nabla\mathbf{d}$. By traversing the entire image,$h(x)$ gets accumulation with the number of 1′s in current pixel difference vector. $\mathbf{H}_D$ changes with difference threshold T_d, and then produces different results with PHE, shown in Fig. 2. A smaller T_d produces result with less contrast enhancement and a bigger T_d obtains a distorted image. To this end, it is necessary to find a suitable threshold T_d to get 2D difference-based histogram.

When $\mathrm{T}_d = 0$, 2D difference-based histogram degenerates into a traditional pixel intensity histogram. 2D difference information for Fig. 3a with different T_d are shown in Fig. 3b. We can learn from Fig. 3b that the difference between 2D difference-based histogram and traditional pixel intensity histogram is that lies in uniformity region, which located on the left side of the blue line in the histogram in Fig. 3b and marked blue in Fig. 3c.

The main cause of distortion is that the range indicates the uniformity region gets widened, as the difference threshold T_d increases. As shown in Fig. 3b, when $\mathrm{T}_d \ge 6$, the range presents uniformity region expanding beyond the blue line. A higher threshold indicates that accumulation of larger difference information is required, but the difference of adjacent pixels in the uniform background region is small. A compromise method is to ensure that the accumulation of background

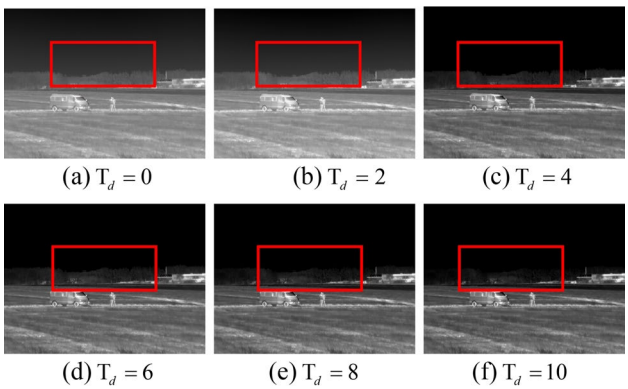

Fig. 2 Enhanced results with different T_d

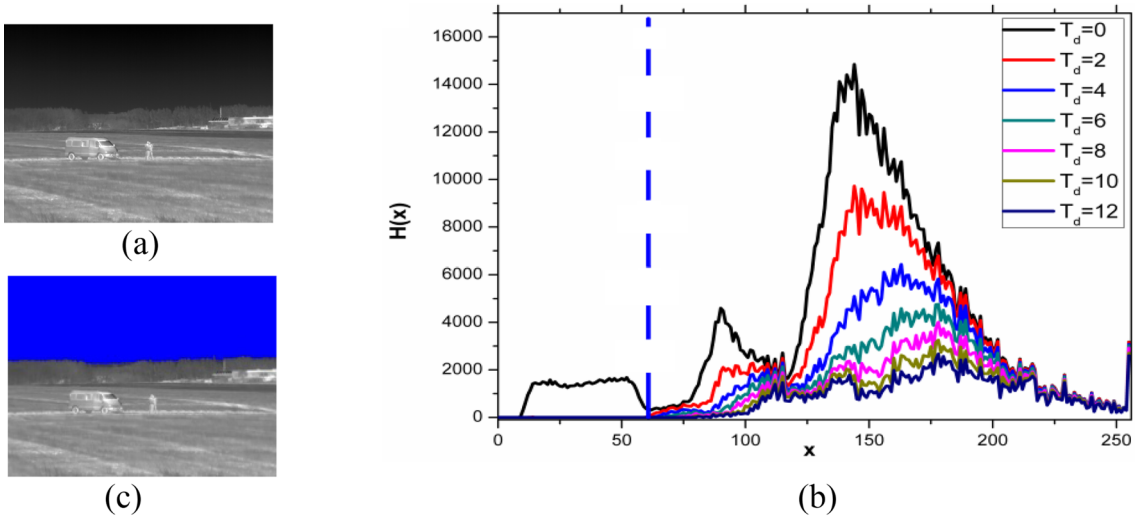

Fig. 3 Original image (**a**), histograms for different T_d(**b**) and image marked background (**c**)

gray levels do not decrease too much when using a higher difference threshold for calculation. In this paper, we apply an improved method based on Ostu [19] to detect background and foreground. Gray-scale density metric Λ is used among $m-1$ ranges which are divided by local valley points m_i in 2D difference-based histogram.

$$\Lambda_{\mathrm{i}} = \frac{C_i}{N_i}, \quad i = 1, 2, \cdots, m-1 \quad , \tag{7}$$

$C_i = \sum_{i=m_i}^{m_i+1} \mathbf{H}_D(I_i)$ and $N_i = m_{i+1} - m_i + 1$ are the cumulative density and gray levels in each range$[m_i,m_{i+1}]$. An adaptive threshold Λ^* is gained by Ostu-based method which exhaustively searches for the optimum as follows:

$$\Lambda^* = \underset{\Lambda_{\min}<\Lambda^*<\Lambda_{\max}}{\operatorname{argmax}} \{\sigma(\Lambda^*)\}, \tag{8}$$

$$\sigma(\Lambda^*) = \varpi_a \cdot (E(\Lambda_a) - \mu_\Lambda)^2 + \varpi_b \cdot (E(\Lambda_b) - \mu_\Lambda)^2, \tag{9}$$

where $E(\Lambda_a)$ and $E(\Lambda_b)$ stand for the mean values of the two separated ranges; μ_Λ is the mean value of a range; and ϖ_a and ϖ_b represent the fractions indicating the component numbers of the two ranges among the whole, respectively.

Then the background region and foreground region can be splitted by such a threshold. For normal intensity histogram, ranges with its grayscale density metric bigger than Λ^* are defined as background and the other ranges are defined as foreground [19].

$$\begin{cases} \Lambda_{0i} \le \Lambda_0^*, & [m_{0i}, m_{0(i+1)}] \in foreground_0 \\ \Lambda_{0i} > \Lambda_0^*, & [m_{0i}, m_{0(i+1)}] \in background_0 \end{cases}, \tag{10}$$

Λ_0^* is the Ostu threshold for intensity histogram, $[m_{0i}, m_{0(i+1)}]$ is ranges, $foreground_0$ and $background_0$ are foreground region and background region.

On the contrary, in 2D difference-based histogram ranges whose grayscale density metric are lower than Λ^* are defined as background.

$$\begin{cases} \Lambda_i \le \Lambda_i^*, & [m_{ii}, m_{i(i+1)}] \in background_i \\ \Lambda_i > \Lambda_i^*, & [m_{ii}, m_{i(i+1)}] \in foreground_i \end{cases}, \tag{11}$$

Λ_i^* is the Ostu threshold for 2D difference-based histogram with difference threshold $T_d = i$.

To obtain proper contrast enhancement without causing any distortion of the output image, we choose the maximum difference threshold T_d by keeping the background area in the difference histogram consistent with the background area in the intensity histogram. The formula is defined as follows:

$$\max_{\forall \mathbb{C}^*} \{T_d\}, \tag{12}$$

$$\mathbb{C}^* = background \le \{background_0 \cup background_i\}. \tag{13}$$

In formula 13, the background calculated based on the 2D difference information includes the uniformity area in the foreground and the background area with concentrated pixel distribution. $\mathbb{C}^*$ means a condition that the background area in the 2D difference-based histogram keeps consistent with the background area in the intensity histogram. T_d T is updated iteratively and stops when the background calculation condition is satisfied.

2.2 Display range supervise

For most HE-based technology, display gray range of output image is the full display range L. They may lack adaptability to different scenes, and background noise in scenes which are uniformity or not complex enough gets enhanced and becomes noticeable. These annoying results have a bad influence on infrared observation and monitoring, the results of HE are shown in Fig. 4.

In this paper, we apply display range supervise for output infrared image using difference information. The principle of range restricted is to control the display range of the output image by connecting the complex scene with the uniform scene through a reasonable curve. There are two steps to achieve display range supervise, assessment of the scenes should be quantified by difference information calculation firstly. Second, the display range of different scenes is obtained by establishing the relationship between the scene evaluation and the defined output display range.

2.2.1 (1) Scene assessment

Image classification is a hot research topic in the field of image processing, and many image classification methods have been produced [20]. However, quantitatively assessing the complexity of an image scene is a challenge. In this manuscript, we try to quantify image scene by difference information calculation. Difference vector of each pixel represents the relationship between a pixel and its neighborhood. Pixels in an image scene with their difference vectors are full of '1′ indicate more textures and edges than pixels difference vectors are full of '0′. We call pixels whose difference vectors are full of '1′ feature pixels. Then we count the number of feature pixels N_D in infrared images.

$$N_D = \begin{cases} +1 & \text{num}(\nabla \mathbf{d}) = 4 \\ 0 & else \end{cases}. \tag{14}$$

It is obvious that N_D is small in a uniformity scene and big in the scene full with textures and edges. Figure 5 shows that feature pixels are marked in red in four different infrared images.

2.2.2 (2) Restrict display range

The number of feature pixels is the specific quantification of infrared scene complexity. Display range of infrared output image can be restricted by these feature pixels. We get output infrared display range by establishing a feature pixels dependent mapping function. To utilize such feature pixels dependent mapping function, the following principles need to be followed: (1) an image scene with few feature pixels classified as an uniformity scene;(2) an image scene with a lot of feature pixels classified as a complexity scene;(3) all images are mapped to a range of 0 to 1 according to their feature pixels. Sigmoid function $Sg(x) = 1/1 + e^{-x}$ meets the above requirements in most cases, as shown in Fig. 6a. We apply an improved mapping function based on the sigmoid function, as shown in (14).

$$\xi(x) = \alpha \cdot (Sg(\omega \cdot x + \theta) + \varphi), \tag{15}$$

α,ω,θ,φ present the amplitude, scale, phase, and shift parameters. Set α=1,φ=0 according to the above requirements. Human visual system has a property of logarithmic to the response to brightness [16]. We apply log function to feature pixels, then $x = \log(N_D+1)$.θ and ω depend on the resolution of infrared images $W \times H$. The phase and scale parameters can be computed as follows according to [19].

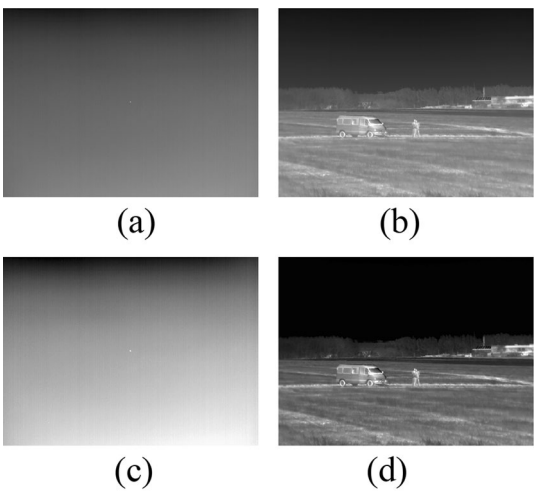

Fig. 4 Original image (**a**, **b**) and enhanced by HE (**c**, **d**)

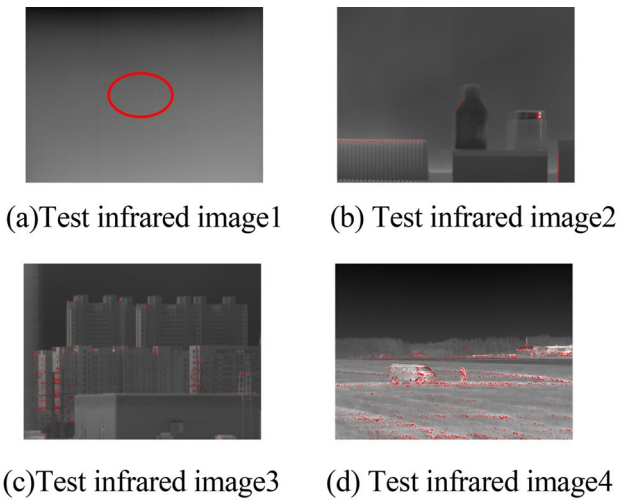

Fig. 5 Infrared images with feature pixels marked in red

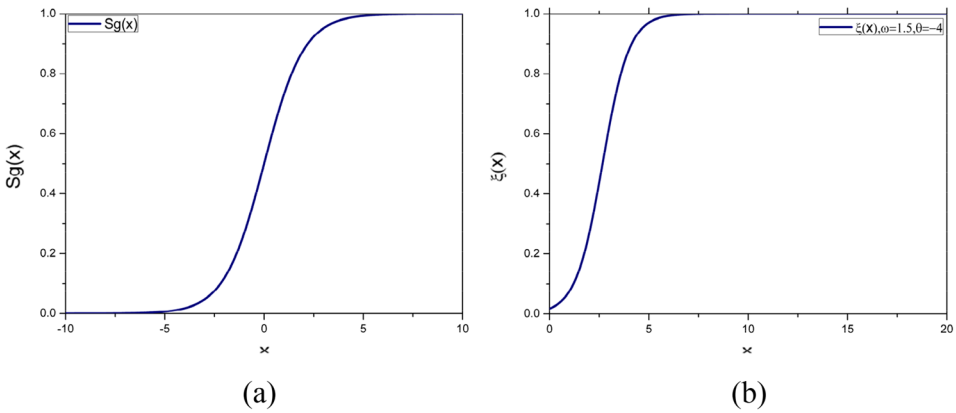

(a) (b)

Fig. 6 Curves of sigmoid function (**a**) and display range mapping function (**b**)

$$\begin{cases} \omega = \dfrac{\ln(\frac{\varepsilon_2}{1-\varepsilon_2} \cdot \frac{1-\varepsilon_1}{\varepsilon_1})}{N_{D\max} - N_{D\min}} \\ \theta = \ln(\frac{\varepsilon_1}{1-\varepsilon_1}) - \omega \cdot N_{D\min} \end{cases}, \tag{16}$$

ε_1 is the minimum valid value of $\xi(x)$, $\varepsilon_1 = \xi(N_{D\min}) \to 0$, and ε_2 is the maximum valid value of $\xi(x)$, $\varepsilon_2 = \xi(N_{D\max}) \to 1$. Take 640×480 infrared images as an example, the biggest value of feature pixels is $N_{D\max} \approx 640 \times 480/2$ and $x = \log(N_{D\max}+1) \approx 5$. There may exist many parameter pairs which meet the requirements, as we pursue a rough mapping of scene classification. One parameter pairs of the scale and phase can be set as ω=1.5 and θ= −4, and its curve shows in Fig. 6b.

The output display range L_R of an infrared image, which needs to be enhanced, is computed as follows:

$$L_R = \xi(x) \cdot (L-1). \tag{17}$$

2.3 Adaptive PHE

Another drawback of HE-based technology is that they easily lead to the combination of small or similar gray values. In other words, if the calculation of some pixel gray values is small, tiny details in their values will be lost. The way they use cumulative methods for information accumulation inevitably leads to the combination of some gray values. To handle this problem, the combination of small or similar gray values should be reduced or eliminated. In this paper, adaptive plateau histogram equalization (APHE) is introduced. The difference between PHE and HE is that PHE has a plateau dominating the upper or lower allowance of histogram; thus, control the combination of gray values.

$$\tilde{h}(x) = \begin{cases} P & h(x) \geq P \\ h(x) & else \end{cases}. \tag{18}$$

Plateau value P has a range from 1 to $W \times H$ in conventional HE. A great number of methods have been proposed to choose plateau value in the past decades [3, 21]. The proposed method uses the calculation of difference information, and it has the same drawback of gray values combination in output image as conventional HE technology.

As a result, a proper plateau value should be selected for protecting details information in the input infrared image. In Sect. 2.1, background and foreground in an infrared image are detected, then the minimum local valley points in foreground can be selected as the plateau value.

$$P = min(m_1, \cdots, m_i, \cdots, m_n) \quad m_i \in foreground\,. \tag{19}$$

2.4 Redefined HE

At last, we redefine the HE technology by changing three factors and formulate as follows:

$$O(m,n) = \max(L_R, L_S) \cdot I(m,n) \cdot \frac{\sum_{t=0}^{i} \tilde{\mathbf{H}}_D(t)}{\sum_{k=0}^{L-1} \tilde{\mathbf{H}}_D(k)}, \tag{20}$$

$\tilde{\mathbf{H}}_D$ presents with 2D difference information and modified by a plateau P.L_R is normalized from 0 to $L-1$. $\max(L_R, L_S)$ guarantees that the original display range is not compressed, L_S is the display range of original infrared image.

3 Experiment and discussion

In this section, we make a lot of comparative experiments for infrared images. Eight experimental infrared images are chosen to test the proposed method, half of them are downloaded from a public database [22] and others are captured from real-owned infrared sensors to test the adaptability of the proposed method. Widely used algorithms and state-of-the-art methods, such as HE, DPHE [3], CLAHE [13], Wavelet [4], MSR [5], LDR [17] and AHPBCM [19], have

been introduced for comparison. The processed comparison results are given in Figs. 7, 8, 9, 10, 11, 12, 13, 14, the calculation results of display range of eight original infrared images are shown in Table 1, related discussions for qualitative evaluation and quantitative assessment are shown below.

3.1 Visual comparisons

First of all, we conduct a qualitative observation. From Figs. 7a to 14a, all original infrared images, which need to be further processed, have low contrast, blurred foreground and unclear edge details. Figures 7b–14b are result images enhanced by HE. HE enhances infrared images contrast without any restrictions, easily leads to over-enhancement and noise amplification. Compared to the original image, the black and white of the result image pixel grayscale is more prominent, but the details are merged. Especially outdoor house in Figs. 9b and 10b, windows in Figs. 11b and 13b, the tires in Figs.12b and 14b. DPHE and CLAHE are both upgrade and improvement of HE-based technology. DPHE has suppressed the shortcomings of HE technology to a certain extent, and the visual experience has been improved, but there are still serious over-enhancement and noise amplification, especially in uniformity region. Figures 7c–14c are enhanced result images by DPHE, they present a more comfortable visual experience than result images enhanced by HE. CLAHE can enhance the contrast and improve the visual perception of infrared image. However, CLAHE is derived from HE technology, the background and foreground in infrared image cannot be distinguished. In most cases, the foreground area with more details is better enhanced, but the contrast between background area and foreground area is less effective. Images from Figs. 7d–14d are processed images by CLAHE. The reason for the good performance of visual perception in Figs. 7d and, 11d–14d is the foreground in the original image has more details and occupies most of the entire image or the foreground is clearly contrasted with the background.

Result image enhanced by Wavelet method is shown in Figs 7e–14e. With the appropriate coefficient selection, Wavelet can enhance the image details considerably, but the contrast of the image is not enhanced, and the related blurred phenomenon of the infrared image is not improved. The MSR method extracts the background radiation part from the infrared image, and adds the obtained multi-scale target foreground radiation to obtain the result image, which can mine many inconspicuous details [5]. In Figs. 8f and 9f, details that are not visible in the original image are highlighted after MSR processed. But for infrared image contains many uniform areas, the contrast enhanced by MSR is limited. As can be seen in Figs. 8f, 10f–14f.

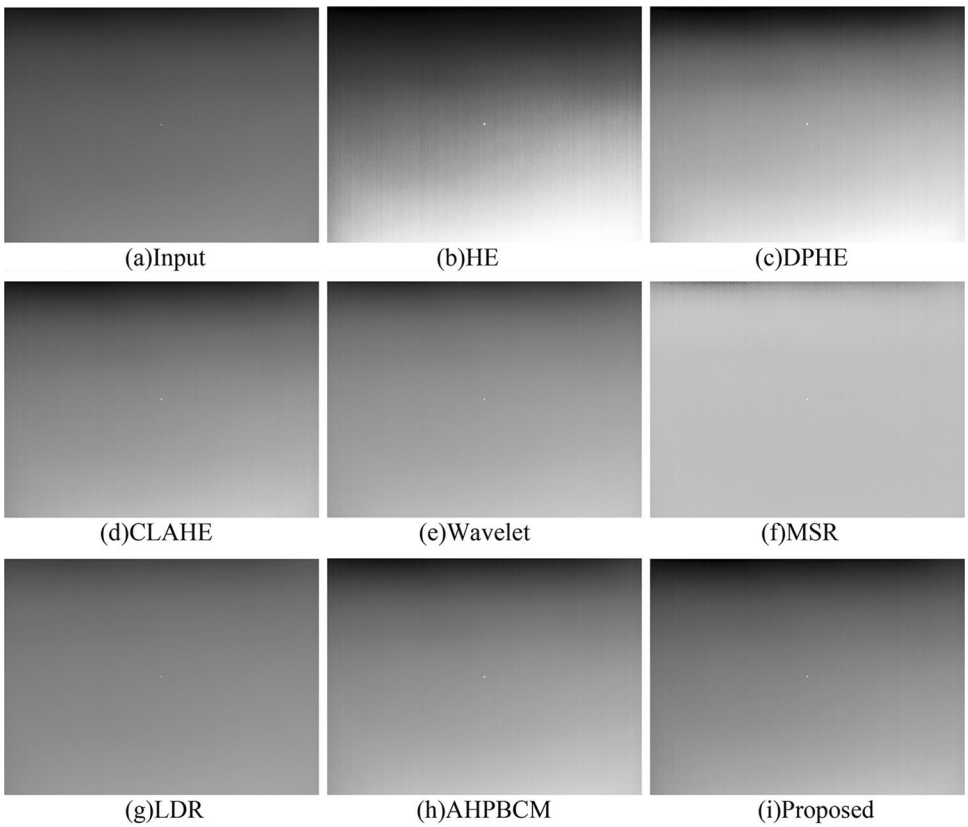

Fig. 7 **a** Image1 and enhanced results by **b** HE, **c** DPHE, **d** CLAHE, **e** Wavelet, **f** MSR, **g** LDR, **h** AHPBCM and **i** proposed method

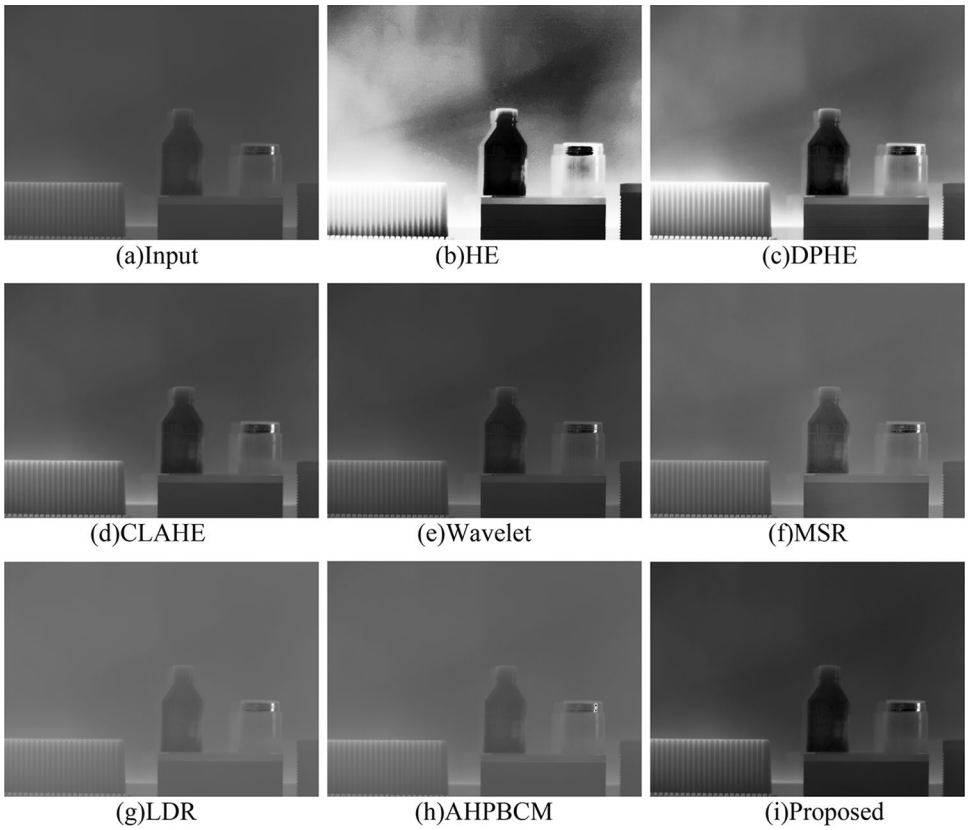

Fig. 8 **a** Image2 and enhanced results by **b** HE, **c** DPHE, **d** CLAHE, **e** Wavelet, **f** MSR, **g** LDR, **h** AHPBCM and **i** proposed method

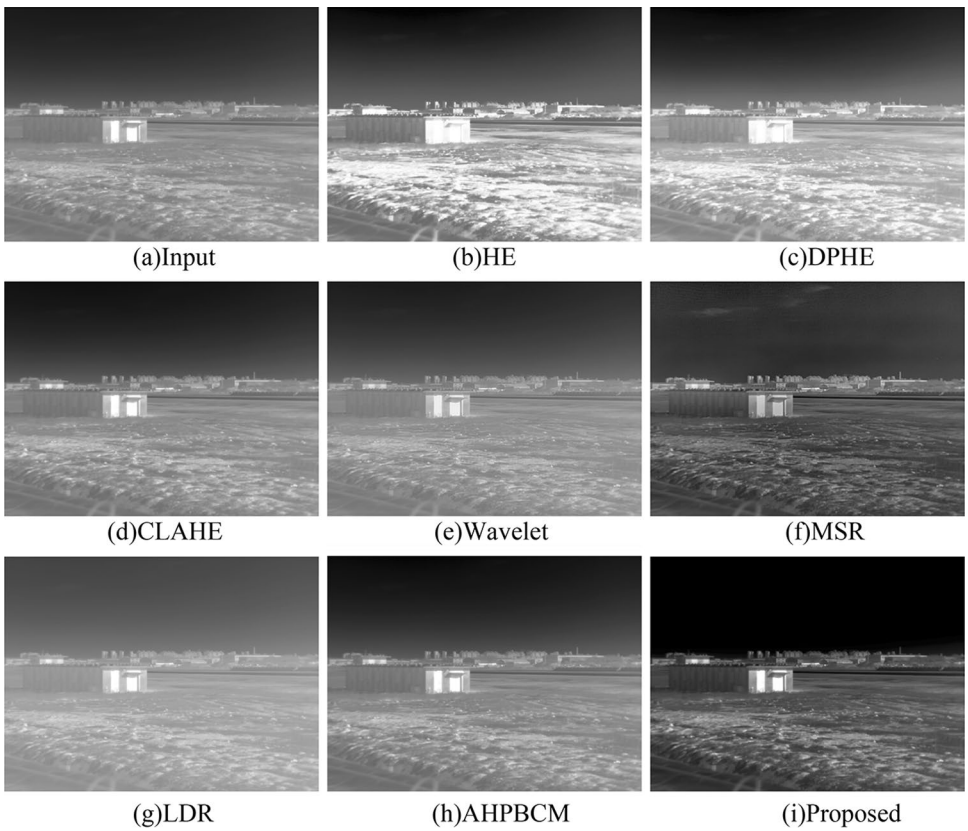

Fig. 9 **a** Image3 and enhanced results by **b** HE, **c** DPHE, **d** CLAHE, **e** Wavelet, **f** MSR, **g** LDR, **h** AHPBCM and **i** proposed method

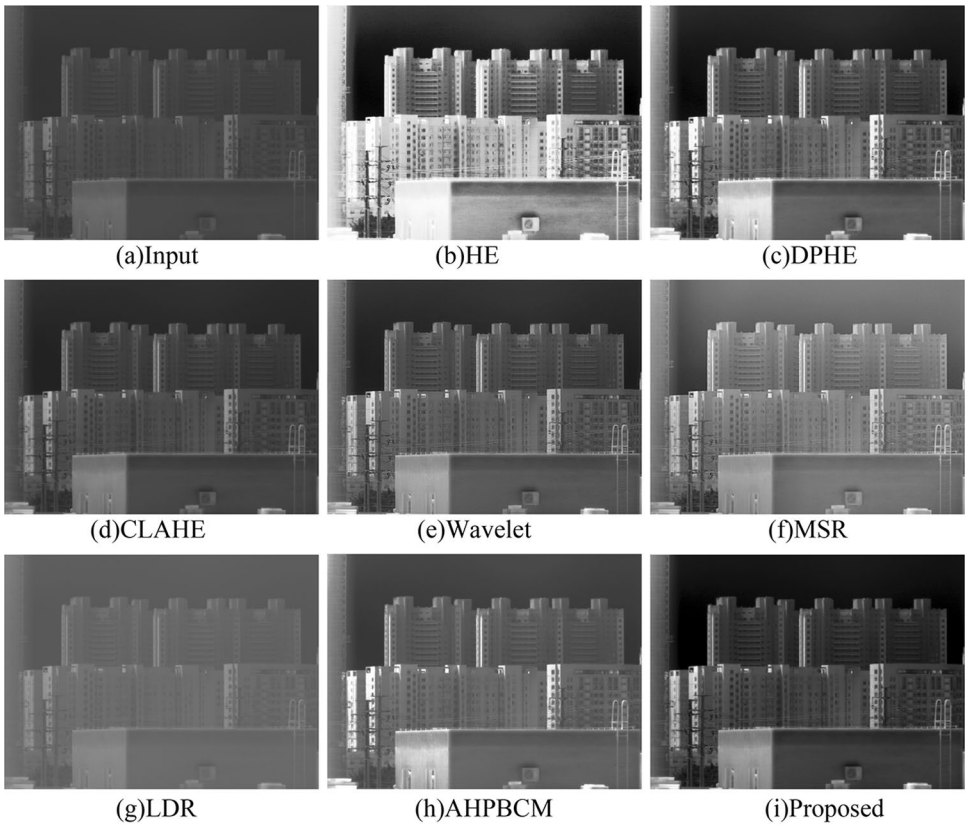

Fig. 10 **a** Image4 and enhanced results by **b** HE, **c** DPHE, **d** CLAHE, **e** Wavelet, **f** MSR, **g** LDR, **h** AHPBCM and **i** proposed method

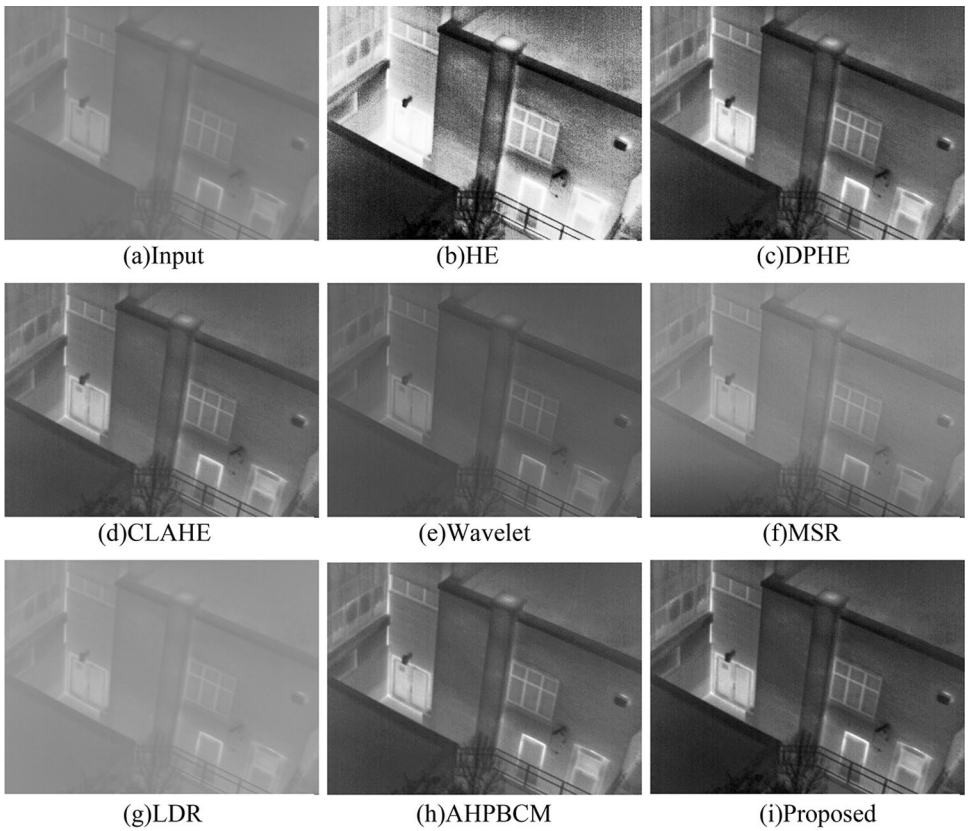

Fig. 11 **a** Image5 and enhanced results by **b** HE, **c** DPHE, **d** CLAHE, **e** Wavelet, **f** MSR, **g** LDR, **h** AHPBCM and **i** proposed method

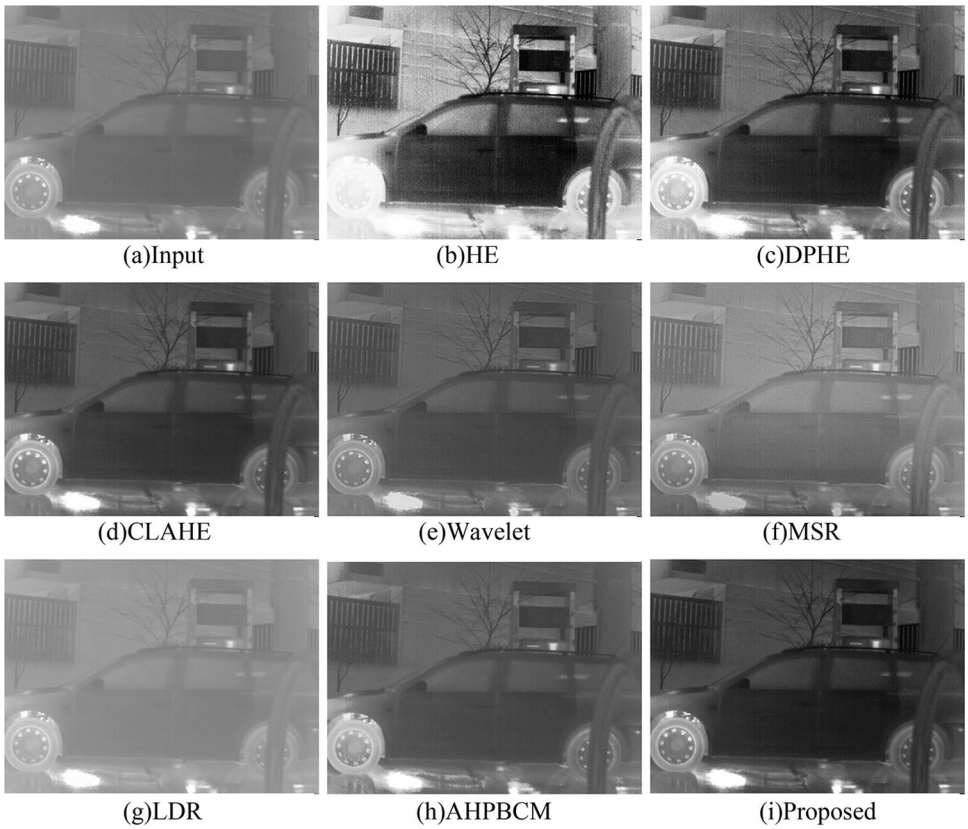

Fig. 12 **a** Image6 and enhanced results by **b** HE, **c** DPHE, **d** CLAHE, **e** Wavelet, **f** MSR, **g** LDR, **h** AHPBCM and **i** proposed method

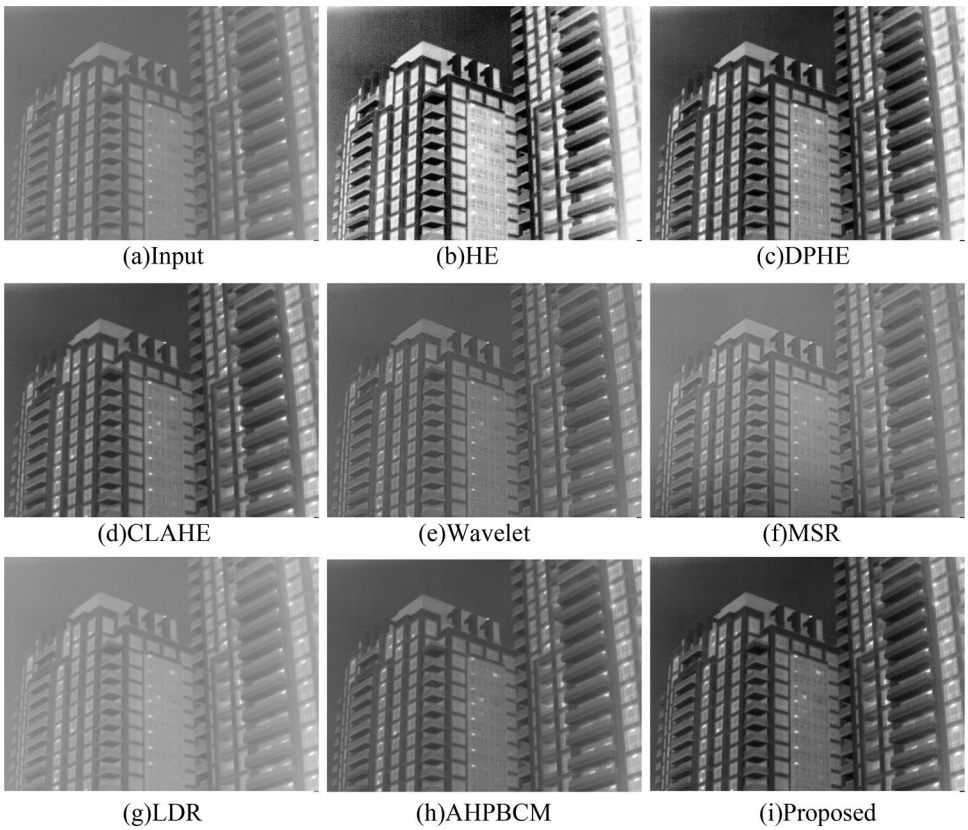

Fig. 13 **a** Image7 and enhanced results by **b** HE, **c** DPHE, **d** CLAHE, **e** Wavelet, **f** MSR, **g** LDR, **h** AHPBCM and **i** proposed method

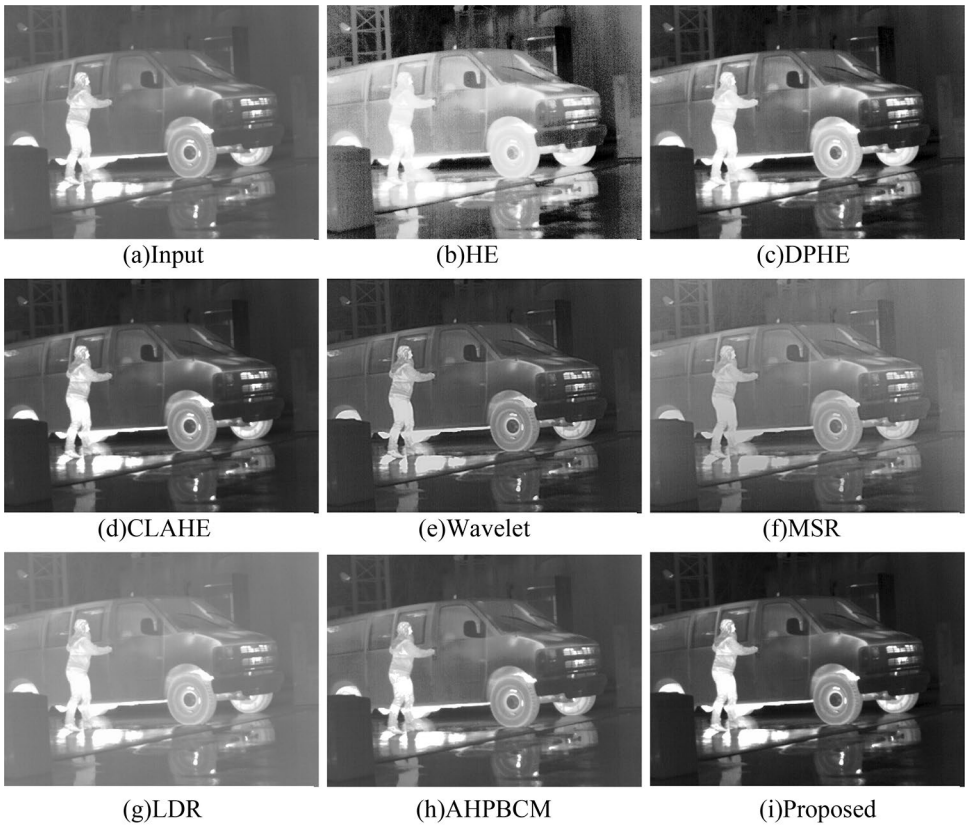

Fig. 14 **a** *Image8* and enhanced results by **b** HE, **c** DPHE, **d** CLAHE, **e** Wavelet, **f** MSR, **g** LDR, **h** AHPBCM and **i** proposed method

Table 1 Display range for output image

	Image1	Image2	Image3	Image4	Image5	Image6	Image7	Image8
N_D	6	29	362	665	683	1575	1144	1364
$\xi(N_D)$	0.054	0.140	0.452	0.557	0.560	0.686	0.639	0.667
L_R	14	36	115	142	143	175	163	170

LDR separates the difference vector for each layer and adds 255 difference vectors to obtain a gray-mapping function. The purpose of LDR is to amplify the difference between the pixels of the original image. But the simply summation of difference vectors between layers results in a strong image correlation, and the visual effect of processed images by LDR becomes less clear. Almost all images become more blurred, although the difference information of the original image is magnified. All result images processed by LDR are present in Figs. 7g–14g.

AHPBCM distinguishes between foreground and background, and uses particle swarm optimization to correct the brightness of the enhanced image. The algorithm performs well in suppressing the problem of over-enhancement and noise amplification in the uniform region of the background. The processed results are shown in Figs. 7h–14h. However, due to its excessive pursuit of balancing the brightness of the original image, the performance is inferior in contrast enhancement.

The advantage of the proposed algorithm is that it not only achieves contrast enhancement and details protecting, but also protects uniformity region from becoming over-enhancement. Infrared image scene in which most areas are uniformity regions is considered to be a 'simple complexity scene'. Figures 7a and 8a can be classified as such kind of scene. Figures 7i and 8i are processed by the proposed method. The contrast between foreground and background is enhanced and the uniformity region in the infrared image background remains intact without over-enhancement and noise amplification. 'Complex scenes' can be defined that the foreground occupies most of the entire infrared image. Figures 12a–14a can be thought of as a so-called 'complex scene'. Figures 12i–14i present the result images processed by the proposed method. Among these results, contrast of the whole image is enhanced and details in foreground is been protected well. The tire in Figs. 12I and 14i and the window on the right side of Fig. 13i are the best proof. The other three experimental

infrared images Figs. 9a–11a are defined as 'Medium complexity scene'. The enhanced images are shown in Figs. 9i–11i, they are excellent in contrast enhancement, details protection and preventing uniformity areas getting over-enhanced compared with other methods. The relevant calculation results of the output display range are shown in Table 1.

We select three regions of different images to enlarge, including uniformity region, less uniformity region and complex region, as shown in Fig. 15. We can learn that HE and DPHE always produce over enhancement and noise amplification, other algorithms will avoid over enhancement or noise amplification, but their processed image contrast and visual perception are not good enough. And the proposed algorithm has better scene adaptability and outperforms other compared algorithms by enhancing the contrast without introducing over-enhancement effect.

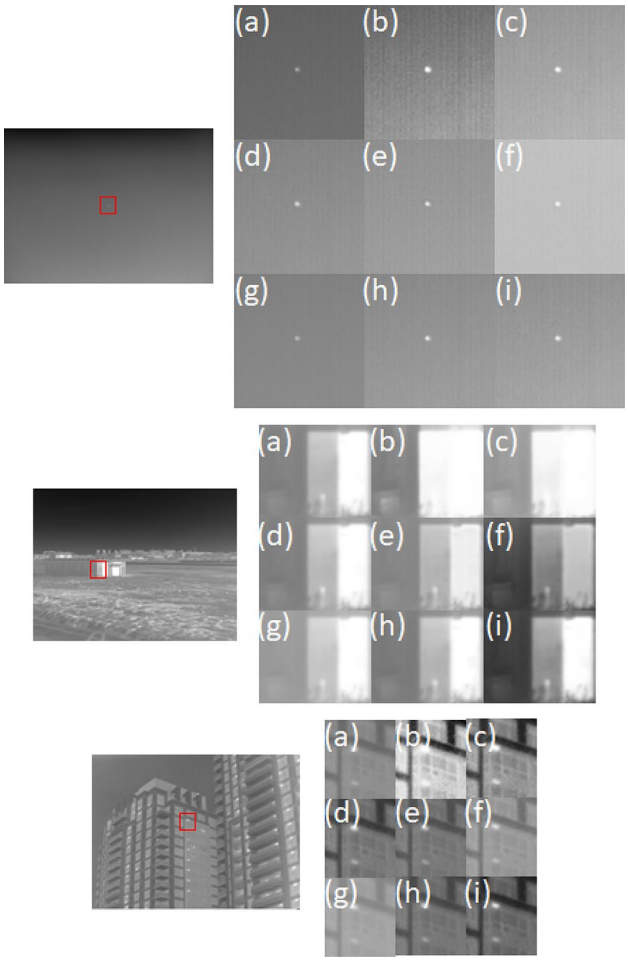

Fig. 15 Enlarged view for part of infrared image 1,3,7, enlarge view are **a** *origin infrared image* and enhanced results by **b** HE, **c** DPHE, **d** CLAHE, **e** Wavelet, **f** MSR, **g** LDR, **h** AHPBCM and **i** proposed method

3.2 Quantitative evaluation

Quantitative evaluation of image enhancement is a tough task because an acceptable criterion by which to quantify the improved perception has yet to be proposed. However, it is desirable to have both quantitative and subjective assessments in practice. For the purpose of further demonstration of the proposed method superiority, we introduce three quantitative metrics: image definition [9], Logarithmic Michelson Contrast Measure [23] and Discrete entropy. Their definitions are as follows:

(1) Image definition Ω is used to reflect the overall performance of the whole enhanced image and a bigger value of Ω meanings that the processed output contains less noises and the enhanced image is more distinct. Consequently, the performance of the corresponding algorithm is better.Ω is defined as follows:

$$\Omega(O) = \frac{PSNR(O)}{\gamma(O)}, \tag{21}$$

γ presents the index of image fuzziness. Its value is widely used to indicate the performance of an enhanced image. The smaller γ value, the lower the degree of image fuzziness. An image with a lower γ value means a clearer displayed image.

$$\gamma(O) = \frac{2}{H * W} \sum_{x=0}^{H-1} \sum_{y=0}^{W-1} \min(p(m,n), 1 - p(m,n)), \tag{22}$$

$$p(m,n) = \sin[\frac{\pi}{2}(1 - \frac{O(m,n)}{MAX})]. \tag{23}$$

MAX represents the maximum gray value that appears in the infrared image.

(2) Logarithmic Michelson Contrast Measure (AME) is employed to represent the performance of local contrast of an enhanced image.

$$AME(O) = -\frac{1}{I_1 * I_2} \sum_{i=1}^{I_1} \sum_{j=1}^{I_2} 20 \cdot \ln(\frac{O_{\max}^{i,j} - O_{\min}^{i,j} + \varepsilon}{O_{\max}^{i,j} + O_{\min}^{i,j} + \varepsilon}), \tag{24}$$

$O_{\max}^{i,j}$ and $O_{\min}^{i,j}$ are the maximum and minimum value in sub-block image with its size $I_1 * I_2$, ε is a minimal number that guarantees the validity of the formula, generally set to ε=10^{-6}.

(3) Discrete entropy (DE) measures the amount of information in an image: a high DE indicates that the image contains more variations and conveys more information.

$$DE = -\sum_{i=0}^{L-1} p_i \log p_i, \tag{25}$$

p_i represents the statistical probability of the existence of a grayscale with a value of i in the infrared image.

The results for each quantitative metric are shown in Fig. 16. The higher the quantitative evaluation index value, the better the performance of the algorithm, except for γ. Although the proposed method can not provide the best performance in all the infrared images, it almost ranks in the top three of all the results. The Wavelet method gets the best scores in 6.483 in DE measures, the proposed method get 6.047, but the contrast of the image enhanced by Wavelet is not improved, and the blurred phenomenon of the infrared image method has not been eliminated. A lower γ means a less fuzziness image. Among all methods, the infrared image enhanced by the proposed method gets lowest score. Therefore, the proposed method gets the second highest score in index of image definition. The top two high scores in AME are HE and RRPDGHE. However, over-enhancement and noise amplification appears in the result images enhanced by HE.

4 Conclusion

In this paper, we present a range-restricted pixel difference global histogram equalization algorithm for infrared image enhancement, which not only achieves contrast enhancement and details protection, but also protects uniformity areas from over-enhancement and noise amplification, thus produces a satisfied subjective quality result. Unlike the traditional histogram which only has intensity information, the proposed method obtains 2D difference-based histogram by calculating difference information between adjacent pixels in a 4-adjacency neighborhood with an adaptive threshold. Then the proposed method redefined the HE technology by

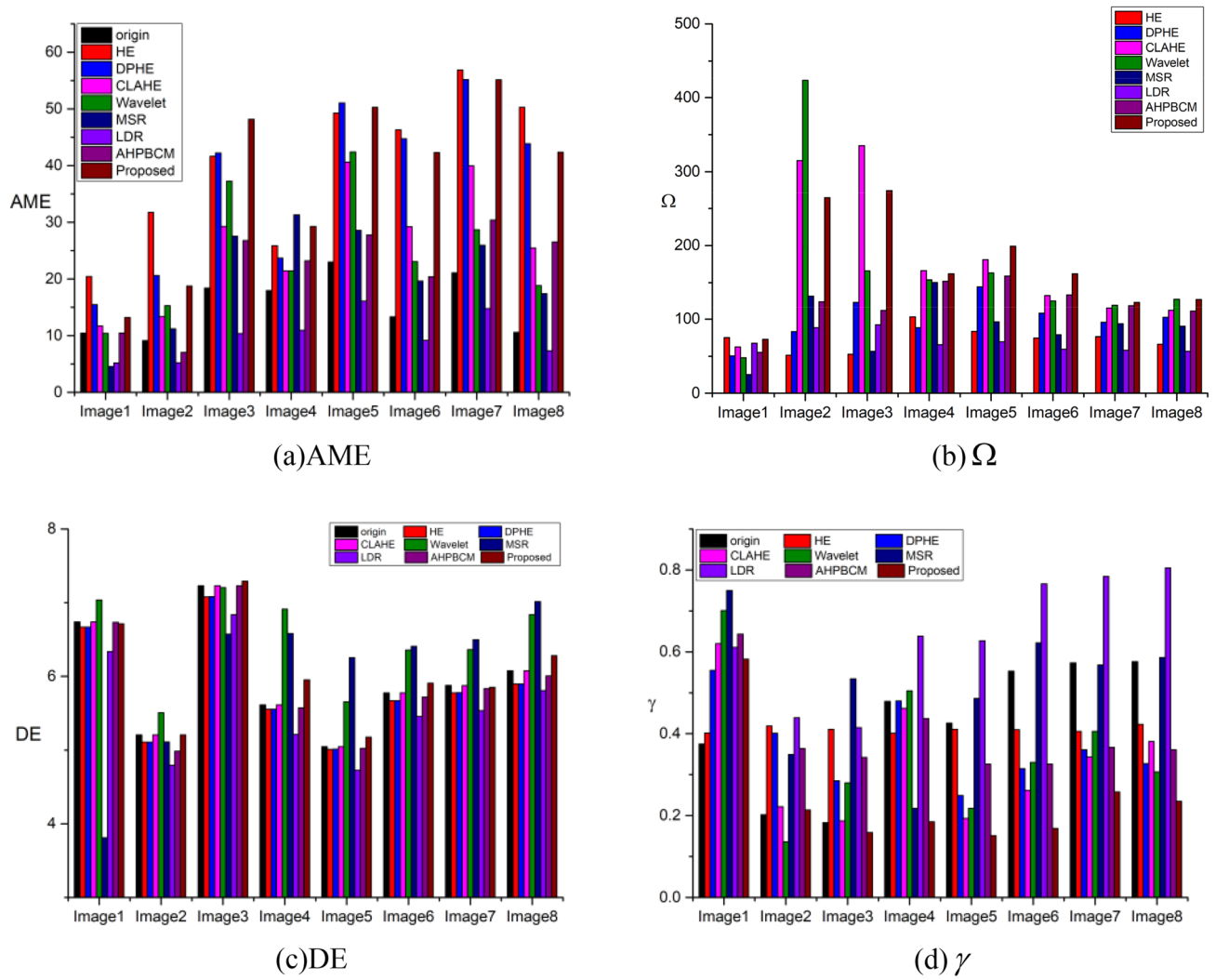

Fig. 16 Quantitative evaluation comparison results using AME, Ω, DE and γ

applying PHE to 2D difference-based histogram instead of intensity histogram. In the new technology, display range for output image is adaptive controlled through a sigmoid function-based curve which related to difference information features, and the local minimum value in the difference histogram representing the foreground is used as a platform value to protect details in original image. Experimental infrared image enhancement results demonstrate that our proposed method is effective in both subjective observation and objective evaluation. In future work, we will optimize and improve to verify the timeliness and applicability of the algorithm.

Funding This work was supported in part by the National Natural Science Foundation of China under Grant number 62001447 and 61705219.

References

1. Viekers, V.E.: Plateau equalization algorithm for real-time display of high-quality infrared imagery. Opt. Eng. **35**, 1921–1926 (1996)
2. Qi, Y., He, R., Lin, H.: Novel infrared image enhancement technology based on the frequency compensation approach. Infrared Phys. Technol. **76**(5), 521–529 (2016)
3. Li, S., Jin, W., Li, L., et al.: An improved contrast enhancement algorithm for infrared images based on adaptive double plateaus histogram equalization. Infrared Phys. Technol. **90**, 164–174 (2018)
4. Liu, T., Zhang, W., Yan, S.: A novel image enhancement algorithm based on stationary wavelet transform for infrared thermography to the de-bonding defect in solid rocket motors. Mech. Syst. Signal. Process. **62–63**, 366–380 (2015)
5. Jang, J.H., Bae, Y., Ra, J.B.: Contrast-enhanced fusion of multisensor images using subband-decomposed multiscale retinex. IEEE Trans. Image Process. **21**(8), 3479–3490 (2012)
6. Zhan, B., Wu, Y.: Infrared image enhancement based on wavelet transformation and retinex. International conference on intelligent human-machine systems and cybernetics. (2010)
7. Rajkumar, S., Dutta, P., Trivedi, A.: Adaptive infrared images enhancement using fuzzy-based concepts [M]. Speech and Language Processing for Human-Machine Communications, pp. 119–128 (2018)
8. Fan, Z., Bi, D., Ding, W.: Infrared image enhancement with learned features[J]. Infrared Phys. Technol. **86**, S1350449517302475 (2017)
9. Bai, X., Zhou, F., Xue, B.: Image enhancement using multi scale image features extracted by top-hat transform. Opt. Laser Technol. **44**(2), 328–336 (2012)
10. Ni, C., Li, Q., Xia, L.Z.: A novel method of infrared image denoising and edge Enhancement. Signal. Process. **88**(6), 1606–1614 (2008)
11. Wang, Y., Pan, Z.: Image contrast enhancement using adjacent-blocks-based modification for local histogram equalization. Infrared. Phys. Technol. **86**(11), 59–65 (2017)
12. Sengee, N., Sengee, A., Choi, H.K.: Image contrast enhancement using bi-histogram equalization with neighborhood metrics. IEEE Trans. Consum. Electron. **56**(4), 2727–2734 (2010)
13. Sonali, S.S., Singh, A.K., Ghrera, S.P., Elhoseny, M.: An approach for de-noising and contrast enhancement of retinal fundus image using CLAHE. Opt. Laser. Technol. **110**(2), 87–98 (2019)
14. Celik, T., Tjahjadi, T.: Contextual and variational contrast enhancement. IEEE Transaction. Image. Process. **12**(20), 3431–3441 (2011)
15. Kim, D., Kim, C.: contrast enhancement using combined 1-D and 2-D histogram-based techniques. IEEE. Signal. Process. Lett. **24**(6), 804–808 (2017)
16. Kim, S.-W., Choi, B.-D., Park, W.-J., Ko, S.-J.: 2D histogram equalization based on the human visual system. Electron. Lett. **22**(6), 443–444 (2016)
17. Lee, C.L., Lee, C., Kim, C.S.: Contrast enhancement based on layered difference representation of 2D histograms. IEEE. Transaction. Image. Process. **20**(12), 5372–5384 (2013)
18. Huang, L., Zhao, W., Sun, Z., Wang, J.: An advanced gradient histogram and its application for contrast and gradient enhancement. J. Vis. Commun. Image R. **31**, 86–100 (2015)
19. Minjie, W., Guohua, G., Weixian, Q., et al.: Infrared image enhancement using adaptive histogram partition and brightness correction. Remote. Sensing. **10**(5), 682–716 (2018)
20. Bosch, A., Zisserman, A., Munoz, X.: Image classification using random forests and Ferns[C]. IEEE 11th international conference on computer vision. IEEE, (2007)
21. Huang, J., Ma, Y., Zhang, Y., et al.: Infrared image enhancement algorithm based on adaptive histogram segmentation. Appl. Opt. **56**(35), 9686–9697 (2017)
22. Database collection of infrared image. Available onl-ine: www.dgp.toronto.edu/nmorris/IR/ (accessed on 31 July 2018)
23. Jaya, V.L., Gopikakumari, R., Jaya, V.L., et al.: IEM: a new image enhancement metric for contrast and sharpness measurements. Int. J. Comput. Appl. **79**(9), 1–9 (2013)